

The stability of the MSW solution to the solar neutrino problem with respect to random matter density perturbations*

Anna Rossi [†],

*Instituto de Física Corpuscular - C.S.I.C.
Departament de Física Teòrica, Universitat de València
46100 Burjassot, València, SPAIN*

Abstract

We present a generalization of the resonant neutrino conversion in matter, including a random component in the matter density profile. The study is focused on the effect of such matter perturbations upon both large and small mixing angle MSW solutions to the solar neutrino problem. This is carried out both for the active-active $\nu_e \rightarrow \nu_{\mu,\tau}$ as well as active-sterile $\nu_e \rightarrow \nu_s$ conversion channels. We find that the small mixing MSW solution is much more stable (especially in δm^2) than the large mixing solution. Future solar neutrino experiments, such as Borexino, could probe solar matter density noise at the few percent level.

* Invited talk presented at “XXXIst Les Rencontres de Moriond- Electroweak Interactions and Unified Theories”, Les Arcs, France - March 16-23, 1996.

This contribution is based on the paper [1] done in collaboration with H. Nunokawa, V. Semikoz and J. W. F. Valle.

[†] E-mail: rossi@evalvx.ific.uv.es, rossi@ferrara.infn.it

1. The comparison among the present experimental results on the observation of the solar neutrinos strongly points to a deficit of neutrino flux (dubbed the Solar Neutrino Problem (SNP)). The most recent averaged data of the chlorine [2], gallium [3, 4] and Kamiokande [5] experiments are:

$$R_{Cl}^{exp} = (2.55 \pm 0.25)\text{SNU}, \quad R_{Ga}^{exp} = (74 \pm 8)\text{SNU}^1, \quad R_{Ka}^{exp} = (0.44 \pm 0.06)R_{Ka}^{BP95} \quad (1)$$

where R_{Ka}^{BP95} is the prediction according to the most recent Standard Solar Model (SSM) by Bahcall-Pinsonneault (BP95)[6].

In particular the SNP is now understood as the strong deficit of the beryllium neutrinos [7]. On the other hand, the high energy boron neutrinos are moderately suppressed, while the low energy ones are almost undepleted. All this seems to imply that any astrophysical solution fails [7, 8] in reconciling the experimental data.

From the particle physics point of view, however, the resonant neutrino conversion due to the neutrino interactions with constituents of the solar material (the Mikheyev-Smirnov-Wolfenstein (MSW) effect) [9] offers the best explanation of the present experimental situation. This scenario provides an extremely good data fit in the small mixing region with $\delta m^2 \simeq 10^{-5}\text{eV}^2$ and $\sin^2 2\theta \simeq 10^{-3} \div 10^{-2}$ [10, 11, 12]. Moreover, the study of the MSW effect has revealed its stability against possible changes of the SSM input parameters [11] especially in the δm^2 parameter.

This talk deals with the stability of the MSW solution with respect to the possible presence of random perturbations in the solar matter density [1].

We remind that in Ref.[13] the effect of periodic matter density perturbations added to a mean matter density ρ upon resonant neutrino conversion was investigated. The major effects show up when the fixed frequency of the perturbation is close to the neutrino oscillation eigenfrequency, and for rather large amplitude values ($\sim 10 \div 20\%$), giving rise to the parametric effects [13]. There are also a number of papers which address similar effects by different approaches [14, 15].

Here we consider the effect of random matter density perturbations $\delta\rho(r)$, characterised by an *arbitrary* wave number k ,

$$\delta\rho(r) = \int dk \delta\rho(k) \sin kr, \quad (2)$$

rather than a periodic or regular perturbation. The effect of solar density as well as solar magnetic field fluctuations upon neutrino spin-flavour conversions has also been considered in Ref. [15], using somewhat different methods.

Moreover, as in Ref.[15], we assume that the perturbation $\delta\rho$ has Gaussian distribution. For small inhomogeneities, the spatial correlation function $\langle \xi^2 \rangle$ can be taken as

$$\langle \delta\rho(r_1)\delta\rho(r_2) \rangle = 2\rho^2 \langle \xi^2 \rangle L_0 \delta(r_1 - r_2), \quad \langle \xi^2 \rangle \equiv \frac{\langle \delta\rho^2 \rangle}{\rho^2}, \quad (3)$$

whose correlation length L_0 obeys the following relation:

$$l_{free} \ll L_0 \ll \lambda_m \quad (4)$$

where $l_{\text{free}} = (\sigma n_0)^{-1}$ is the mean free path of the electrons in the solar medium², and λ_m is the neutrino matter wave length. The lower bound, is dictated by the hydro-dynamical approximation used later, whereas the upper bound expresses the fact that the scale of fluctuations should be much smaller than λ_m (the characteristic neutrino propagation length scale), as indeed the Eq. (3) requires. For the sake of discussion, in the following we choose to adjust L_0 as follows:

$$L_0 = 0.1 \times \lambda_m. \quad (5)$$

The SSM in itself cannot account for the existence of density perturbations, since it is based on hydrostatic evolution equations. On the other hand, the present helioseismology observations cannot exclude the existence of few percent level of matter density fluctuations [16, 17]. Therefore, in what follow we assume, on phenomenological grounds, such levels for ξ , up to 8%.

Before generalizing the MSW scenario, accounting for the presence in the interior of the sun of such matter density fluctuations, first we give a quick reminder to the main features of the MSW effect.

2. The resonant conversion of neutrinos in a matter background is due to the coherent neutrino scattering off matter constituents [9]. This determines an effective matter potential V for neutrinos. In the rest frame of the unpolarised matter, the potential is given, in the framework of the Standard Model, by

$$V = \frac{\sqrt{2}G_F}{m_p} \rho Y \quad (6)$$

where G_F is the Fermi constant and Y is a number which depends on the neutrino type and on the chemical content of the medium. More precisely, $Y = Y_e - \frac{1}{2}Y_n$ for the ν_e state, $Y = -\frac{1}{2}Y_n$ for ν_μ and ν_τ and $Y = 0$ for the sterile ν_s state, where $Y_{e,n}$ denotes the electron and neutron number per nucleon. Let us note the dependence of V on the matter density ρ for which one usually consider the *smooth* distribution, as given by the SSM [6, 18, 19].

Once assumed that there exists a non-vanishing mass difference δm^2 between two different neutrino states and a non-vanishing neutrino mixing θ in vacuum, the neutrinos ν_e 's, created in the inner region of the sun, where the ρ distribution is maximal, can be completely converted into ν_y ($y = \mu, \tau$ or s), while travelling to the solar surface.

This requires two conditions [9]:

1) - the resonance condition. Neutrinos of given energy E experience the resonance if the energy splitting in the vacuum $\delta m^2 \cos 2\theta / 2E$ is compensated by the effective matter potential difference $\Delta V_{ey} = V_e - V_y$. It is helpful to define the following dynamical factor A_{ey}

$$A_{ey}(r) = \frac{1}{2} [\Delta V_{ey}(r) - \frac{\delta m^2}{2E} \cos 2\theta] \quad (7)$$

which vanishes at the resonance, $A_{ey} = 0$. This condition determines the value $\rho_{res} = (m_p \cos 2\theta / 2\sqrt{2}G_F)(Y_e - Y_y)\delta m^2 / E$ which, in turn, implies a resonance layer Δr .

² For Coulomb interactions, the cross-section σ is determined by the classical radius of electron $r_{0e} = e^2/m_e c^2 \sim 2 \times 10^{-13}$ cm, resulting in $l_{\text{free}} \sim 10$ cm for a solar mean density $n_0 \sim 10^{24}$ cm⁻³.

2) - The adiabatic condition. At the resonance layer, the neutrino conversion $\nu_e \rightarrow \nu_y$ is efficient if the propagation is adiabatic. This can be nicely expressed requiring that the neutrino wavelenght λ_m be smaller than Δr [9],

$$\begin{aligned}\alpha_r &= \Delta r / (\lambda_m)_{res} \equiv \frac{\delta m^2 \sin^2 2\theta R_0}{4\pi E \cos 2\theta} > 1, \quad R_0 \approx 0.1 R_\odot, \\ \lambda_m &= \frac{\pi}{\sqrt{A_{ey}^2 + (\delta m^2)^2 \sin^2 2\theta / 16E^2}}, \quad \Delta r = 2\rho_{res} \tan 2\theta |d\rho/dr|^{-1}.\end{aligned}\tag{8}$$

2. Now we re-formulate the evolution equation for the neutrino accounting for a fluctuation term $\delta\rho$ superimposed to the main profile ρ . The perturbation level $\xi = \frac{\delta\rho}{\rho}$ induces a corresponding random component for the matter potential of the form $\Delta V_{ey}\xi$. The evolution for the $\nu_e - \nu_y$ system is governed by

$$i \frac{d}{dt} \begin{pmatrix} \nu_e \\ \nu_y \end{pmatrix} = \begin{pmatrix} H_e & H_{ey} \\ H_{ey} & H_y \end{pmatrix} \begin{pmatrix} \nu_e \\ \nu_y \end{pmatrix},\tag{9}$$

where the entries of the Hamiltonian matrix are given by

$$\begin{aligned}H_e &= 2[A_{ey}(t) + \tilde{A}_{ey}(t)], \quad H_y = 0, \quad H_{ey} = \frac{\delta m^2}{4E} \sin 2\theta, \\ A_{ey}(t) &= \frac{1}{2}[\Delta V_{ey}(t) - \frac{\delta m^2}{2E} \cos 2\theta], \quad \tilde{A}_{ey}(t) = \frac{1}{2}\Delta V_{ey}(t)\xi\end{aligned}\tag{10}$$

Here the matter potential for the active-active $\nu_e \rightarrow \nu_{\mu,\tau}$ conversion reads

$$\Delta V_{e\mu(\tau)}(t) = \frac{\sqrt{2}G_F}{m_p} \rho(t)(1 - Y_n)\tag{11}$$

or alternatively in case $\nu_e \rightarrow \nu_s$

$$\Delta V_{es}(t) = \frac{\sqrt{2}G_F}{m_p} \rho(t)(1 - \frac{3}{2}Y_n)\tag{12}$$

(the neutral matter relation $Y_e = 1 - Y_n$ has been used).

The above system can be rewritten in terms of the following equations:

$$\begin{aligned}\dot{P}(t) &= 2H_{ey}I(t) \\ \dot{R}(t) &= -H_e(t)I(t) \\ \dot{I}(t) &= H_e(t)R(t) - H_{ey}(2P(t) - 1)\end{aligned}\tag{13}$$

where $P = |\nu_e|^2$ is the ν_e survival probability, $R \equiv \text{Re}(\nu_y \nu_e^*)$ and $I \equiv \text{Im}(\nu_y \nu_e^*)$ with the corresponding initial conditions $P(t_0) = 1$, $I(t_0) = 0$, $R(t_0) = 0$. The Eqs. (13) have to be averaged (see [1] for more details) over the random density distribution, taking into account that for the random component we have:

$$\langle \tilde{A}_{ey}^{2n+1} \rangle = 0, \quad \langle \tilde{A}_{ey}(t) \tilde{A}_{ey}(t_1) \rangle = \kappa \delta(t - t_1),\tag{14}$$

$$\kappa(t) = \langle \tilde{A}_{ey}^2(t) \rangle L_0 = \frac{1}{2} \Delta V_{ey}^2(t) \langle \xi^2 \rangle L_0.\tag{15}$$

The noise-averaged version of the system (13) reads as :

$$\begin{aligned}
\dot{\mathcal{P}}(t) &= 2H_{ey}\mathcal{I}(\sqcup) \\
\dot{\mathcal{R}}(t) &= -2A_{ey}(t)\mathcal{I}(\sqcup) - \epsilon\kappa(\sqcup)\mathcal{R}(\sqcup) \\
\dot{\mathcal{I}}(t) &= 2A_{ey}(t)\mathcal{R}(\sqcup) - \epsilon\kappa(\sqcup)\mathcal{I}(\sqcup) - \mathcal{H}_{\uparrow\downarrow}(\epsilon\mathcal{P}(\sqcup) - \infty).
\end{aligned}
\tag{16}$$

where clearly $\langle P(t) \rangle = \mathcal{P}(\sqcup)$, $\langle R(t) \rangle = \mathcal{R}(\sqcup)$, $\langle I(t) \rangle = \mathcal{I}(\sqcup)$. As expected the system of equations (16) explicitly exhibits the noise parameter κ .

It is now possible to envisage the main effects due to the presence of the random field $\delta\rho$ upon the MSW scenario. Now the “ dynamics ” is governed by one more quantity i.e. the noise parameter κ , besides the factor A_{ey} . Actually, the quantity κ can be given the meaning of energy quantum associated with the matter density perturbation. However, let us note that the MSW resonance condition, i.e. $A_{ey}(t) = 0$ remains unchanged, due to the random nature of the matter perturbations. The comparison between the noise parameter κ in Eq. (15) and $A_{ey}(t)$ shows that $\kappa(t) < A_{ey}(t)$, for $\xi \lesssim$ few %, except at the resonance region. As a result, the density perturbation can have its maximal effect just at the resonance. Furthermore, one can find the analogous of condition 2) (see Eq. (8) for the noise to give rise to sizeable effects. Since the noise term gives rise to a damping term in the system (16), it follows that the corresponding noise length scale $1/\kappa$ be much smaller than the thickness of the resonance layer Δr . In other words, the following *adiabaticity* condition

$$\tilde{\alpha}_r = \Delta r \kappa_{res} > 1, \tag{17}$$

is also necessary. There is a simple relation between the two adiabaticity parameters α_r (cfr. (8)) and $\tilde{\alpha}_r$:

$$\tilde{\alpha}_r \approx \alpha_r \frac{\xi^2}{\tan^2 2\theta}. \tag{18}$$

For the range of parameters we are considering, $\xi \sim 10^{-2}$ and $\tan^2 2\theta \geq 10^{-3} - 10^{-2}$, and due to the r.h.s of (4), there results $\tilde{\alpha}_r \leq \alpha_r$. This relation can be rewritten as $\kappa_{res} < \delta H_{res}$, where δH_{res} is the level splitting between the energies of the neutrino mass eigenstates at resonance. This shows that the noise energy quantum is unable to “excite” the system, causing the level crossing (even at the resonance) [13]. In other words, it never violates the MSW adiabaticity condition. From Eq. (18) it follows also that, in the adiabatic regime $\alpha_r > 1$, the smaller the mixing angle value the larger the effect of the noise. Finally, as already noted above, the MSW non-adiabaticity $\alpha_r < 1$ is always transmitted to $\tilde{\alpha}_r < 1$. As a result, under our assumptions the fluctuations are expected to be ineffective in the non-adiabatic MSW regime.

3. All this preliminary discussion is illustrated in the Fig. 1. For definiteness we take BP95 SSM [6] as reference model. We plot \mathcal{P} as a function of $E/\delta m^2$ for different values of the noise parameter ξ . For comparison, the standard MSW case $\xi = 0$ is also shown (lower solid curve). One can see that in both cases of small and large mixing (Fig. 1a and Fig. 1b, respectively), the effect of the matter density noise is to raise the bottom of the pit (see dotted and dashed curves). For example, the enhancement of the survival probability can easily reach 20% for ξ values as small as 4%. In other words, the noise weakens the MSW suppression in the adiabatic-resonant regime, whereas its effect is negligible in the non-adiabatic region, in complete agreement with the results of Ref.[15]. The relative increase of

the survival probability \mathcal{P} is larger for the case of small mixing (Fig. 1a) as already guessed on the basis of Eq. (18). We have also drawn pictorially (solid vertical line) the position, in the \mathcal{P} profile, where ${}^7\text{Be}$ neutrinos fall in for the relevant $\delta m^2 \sim 10^{-5} \text{ eV}^2$, to visualize that these intermediate energy neutrinos are the ones most likely to be affected by the matter noise.

4. Let us analyse the possible impact of this scenario in the determination of solar neutrino parameters from the experimental data. For that we have performed the standard χ^2 fit in the $(\sin^2 2\theta, \delta m^2)$ parameter space. The results of the fitting are shown in Fig. 2 where the 90% confidence level (C.L.) areas are drawn for different values of ξ . Fig. 2a and Fig. 2b refer to the cases of $\nu_e \rightarrow \nu_{\mu,\tau}$ and $\nu_e \rightarrow \nu_s$ conversion, respectively. One can observe that the small-mixing region is almost stable, with a slight shift down of δm^2 values and a slight shift of $\sin^2 2\theta$ towards larger values. The large mixing area is also pretty stable, exhibiting the tendency to shift to smaller δm^2 and $\sin^2 2\theta$. The smaller δm^2 values compensate for the weakening of the MSW suppression due to the presence of matter noise, so that a larger portion of the neutrino energy spectrum can be converted. The $\xi = 8\%$ case, considered for the sake of demonstration, clearly shows that the small mixing region is much more stable than the large mixing one even for such large value of the noise. Moreover the strong selective ${}^7\text{Be}$ neutrino suppression, which is the nice feature of the MSW effect, is somewhat degraded by the presence of matter noise. Consequently the longstanding conflict between chlorine and Kamiokande data is exacerbated and the data fit gets worse. Indeed, the presence of the matter density noise makes the data fit a little poorer: $\chi_{min}^2 = 0.1$ for $\xi = 0$, it becomes $\chi_{min}^2 = 0.8$ for $\xi = 4\%$ and even $\chi_{min}^2 = 2$ for $\xi = 8\%$ for the $\nu_e \rightarrow \nu_{\mu,\tau}$ transition.

The same tendency is met in the case of transition into a sterile state (Fig. 2b): $\chi_{min}^2 = 1$ for $\xi = 0$, it becomes $\chi_{min}^2 = 3.6$ for $\xi = 4\%$ and $\chi_{min}^2 = 9$ for $\xi = 8\%$.

In conclusion we have shown that the MSW solution to the SNP exists for any realistic levels of matter density noise ($\xi \leq 4\%$). Moreover the MSW solution is essentially stable in mass ($4 \cdot 10^{-6} \text{ eV}^2 < \delta m^2 < 10^{-5} \text{ eV}^2$ at 90% CL), whereas the mixing appears more sensitive to the level of fluctuations.

5. We can reverse our point of view, wondering whether the solar neutrino experiments can be a tool to get information on the the level of matter noise in the sun. In particular, the future Borexino experiment [20], aiming to detect the ${}^7\text{Be}$ neutrino flux could be sensitive to the presence of solar matter fluctuations. In the relevant MSW parameter region for the noiseless case, the Borexino signal cannot be definitely predicted (see Fig. 3a). Within the present allowed C.L. regions (dotted line) the expected rate, $Z_{Be} = R_{Be}^{pred} / R_{Be}^{BP95}$ (solid lines), is in the range $0.2 \div 0.7$.

On the other hand, when the matter density noise is switched on, e.g. $\xi = 4\%$ (see Fig. 3b), the minimal allowed value for Z_{Be} becomes higher, $Z_{Be} \geq 0.4$. Hence, if the MSW mechanism is responsible for the solar neutrino deficit and Borexino experiment detects a low signal, say $Z_{Be} \lesssim 0.3$ (with good accuracy) this will imply that a 4% level of matter fluctuations in the central region of the sun is unlikely. The same argument can be applied to $\nu_e \rightarrow \nu_s$ resonant conversion, whenever future large detectors such as Super-Kamiokande and/or the Sudbury Neutrino Observatory (SNO) establish through, e.g. the measurement of the charged to neutral current ratio, that the deficit of solar neutrinos is due to this kind of

transition. The expected signal in Borexino is very small $Z_{Be} \approx 0.02$ for $\xi = 0$ (see Fig. 3c). On the other hand with $\xi = 4\%$, the minimum expected Borexino signal is 10 times higher than in the noiseless case, so that if Borexino detects a rate $Z_{Be} \lesssim 0.1$ (see Fig. 3d) this would again exclude noise levels above 4%.

Let us notice that Super-Kamiokande and SNO experiments, being sensitive only to the higher energy Boron neutrinos, probably do not offer similar possibility to probe such matter fluctuations in the sun.

The previous discussion, which certainly deserves a more accurate analysis involving also the theoretical uncertainties in the ${}^7\text{Be}$ neutrino flux, shows the close link between neutrino physics and solar physics.

It is a pleasure to thank N. Yahlali and H. Nunokawa for reading the manuscript. This work has been supported by the grant N. ERBCHBI CT-941592 of the Human Capital and Mobility Program.

References

- [1] H. Nunokawa, A. Rossi, V. Semikoz and J. W. F. Valle, preprint FTUV/95-47, IFIC/95-49, hep-ph/9602307, accepted for the publication in *Nucl. Phys. B*.
- [2] B.T. Cleveland *et al.*, *Nucl. Phys. B (Proc. Suppl.)* **38** (1995) 47.
- [3] GALLEX Collaboration, P. Anselmann *et al.*, LNGS Report 95/37 (June 1995).
- [4] SAGE Collaboration, J.S. Nico *et al.*, *Proc. 27th Conf. on High Energy Physics*, Glasgow, UK (July 1994).
- [5] Y. Suzuki, *Nucl. Phys. B (Proc. Suppl.)* **B38** (1995) 54
- [6] J. N. Bahcall and R. K. Ulrich, *Rev. Mod. Phys.* **60** (1990) 297;
J. N. Bahcall and M. H. Pinsonneault, *Rev. Mod. Phys.* **64** (1992) 885;
J. N. Bahcall and M. H. Pinsonneault, preprint IASSNS-AST 95/24
- [7] V. Castellani, *et al Phys. Lett.* **B324** (1994) 245;
N. Hata, S. Bludman, and P. Langacker, *Phys. Rev.* **D49** (1994) 3622;
V. Berezinsky, *Comments on Nuclear and Particle Physics* **21** (1994) 249;
J. N. Bahcall, *Phys. Lett.* **B338** (1994) 276.
- [8] V. Berezinsky, G. Fiorentini and M. Lissia, *Phys. Lett.* **B365** (1996) 185.
- [9] S. P. Mikheyev and A. Yu. Smirnov, *Sov. J. Nucl. Phys.* **42** (1986) 913;
Sov. Phys. Usp. **30** (1987) 759;
L. Wolfenstein, *Phys. Rev.* **D17** (1978) 2369; *ibid.* **D20** (1979) 2634.

- [10] G. Fiorentini *et al.* *Phys. Rev.* **D49** (1994) 6298;
N. Hata and P. Langacker, *Phys. Rev.* **D50** (1994) 632.
- [11] P. I. Krastev and A. Yu. Smirnov, *Phys. Lett.* **B338** (1994) 282;
V. Berezhinsky, G. Fiorentini and M. Lissia, *Phys. Lett.* **B341** (1994) 38.
- [12] E. Calabresu *et al.*, *Phys. Rev.* **D53** (1996) 4211;
J. N. Bahcall and P. I. Krastev, Princeton preprint IASSNS-AST 95/56,
hep-ph/9512378
- [13] P. I. Krastev and A. Yu Smirnov, *Phys. Lett.* **B226** (1989) 341; *Mod.*
Phys. Lett. **A6** (1991) 1001.
- [14] A. Schafer and S. E. Koonin, *Phys. Lett.* **B185** (1987) 417;
R. F. Sawyer, *Phys. Rev.* **D42** (1990) 3908;
A. Abada and S.T. Petcov, *Phys. Lett.* **B279** (1992) 153.
- [15] F. N. Loreti and A. B. Balantekin, *Phys. Rev.* **D50** (1994) 4762.
- [16] J. Christensen-Dalsgaard, private communication.
- [17] P. Kumar, E. Quataert, and J. N. Bahcall, astro-ph/9512091
- [18] S. Turck-Chiéze and I. Lopes, *Ap. J.* **408** (1993) 346;
S. Turck-Chiéze *et al.*, *Phys. Rep.* **230** (1993) 57.
- [19] V. Castellani, S. Degl'Innocenti and G. Fiorentini, *Astron. Astrophys.*
271 (1993) 601.
- [20] C. Arpesella *et al.* (Borexino Collaboration), Proposal of BOREXINO
(1991).

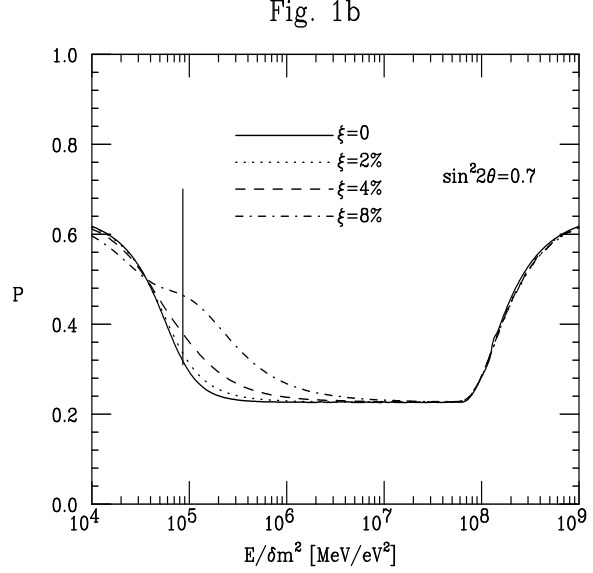
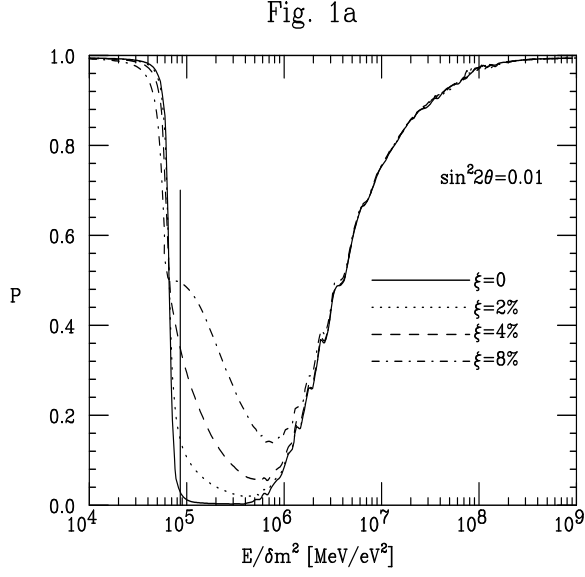


Fig. 1: The averaged solar neutrino survival probability P versus $E/\delta m^2$ for small mixing angle, $\sin^2 2\theta = 0.01$, (Fig. 1a) and for large mixing angle, $\sin^2 2\theta = 0.7$, (Fig. 1b). The different curves refer to different values of matter noise level ξ as indicated.

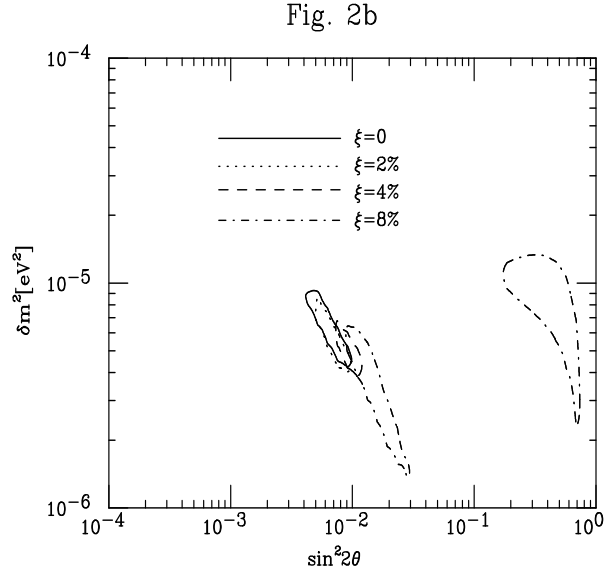
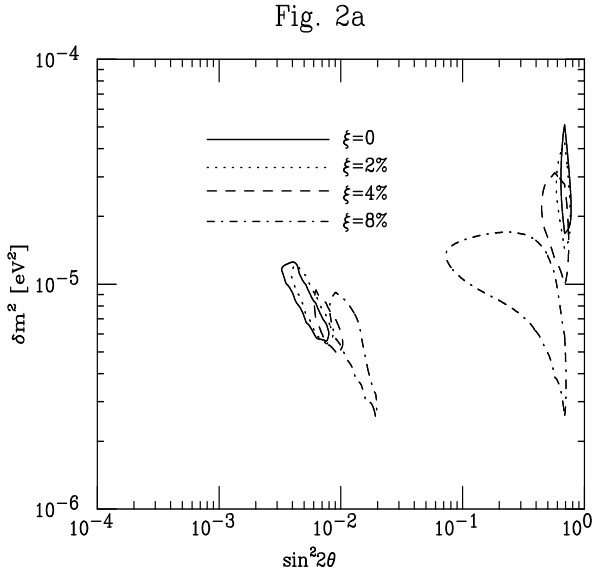


Fig. 2: The 90% C.L. allowed regions for the $\nu_e \rightarrow \nu_{\mu,\tau}$ (Fig. 2a) and for the $\nu_e \rightarrow \nu_s$ (Fig. 2b) conversion. The different curves refer to different values of matter noise level ξ as indicated.

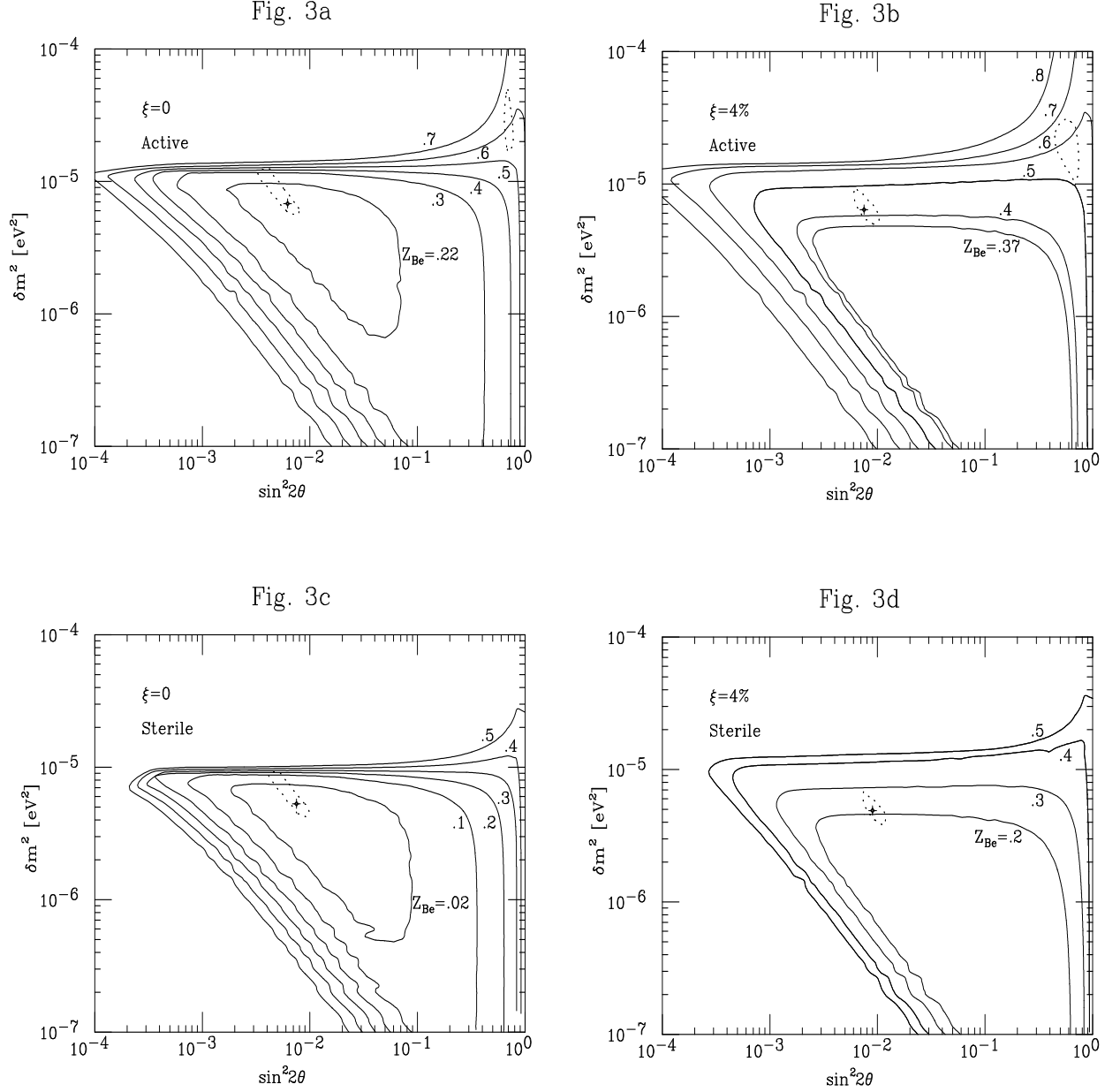


Fig. 3: The iso $Z_{Be} = R_{Be}^{pred}/R_{Be}^{BP95}$ contours (figures at curve) in the $\nu - e$ scattering Borexino detector (solid lines). The threshold energy for the recoil electron detection is 0.25 MeV. The 90% C.L. regions (dotted line) and the corresponding best fit point are also drawn. Fig. 3a and Fig. 3b refer to the case of $\nu_e \rightarrow \nu_{\mu,\tau}$ conversion and for $\xi = 0$ and $\xi = 4\%$, respectively. Fig. 3c and Fig. 3d refer to the case of $\nu_e \rightarrow \nu_s$ conversion and for $\xi = 0$ and $\xi = 4\%$, respectively.